Model Studies of the Glyoxalase I Reaction. Buffer-catalysed Rearrangement to α-Hydroxyacyl Thiolesters of Hemithioacetals from 2-Mercaptoethanol with Substituted Arylglyoxals

Kenneth T. Douglas* and Husniye Demircioglu
Department of Chemistry, University of Essex, Colchester, Essex CO4 3SQ

A model system for the reaction catalysed by the enzyme glyoxalase I has been studied kinetically. A series of substituted arylglyoxals was synthesised. The hemithioacetals formed between these α-ketoaldehydes and β-mercaptoethanol in aqueous solutions at pH 9.2 underwent smooth rearrangement to the corresponding α-hydroxyacyl thiolester. The kinetics of this rearrangement were studied anaerobically and rate constants showed saturation dependence on thiol concentration $\{k_{obs} = k_{max.} K_h[RSH]/(1 + K_h[RSH])\}$, where $k_{max.}$ refers to the limiting value of k_{obs} at high thiol concentrations and K_h is the equilibrium constant for the hemithioacetal equilibrium. The rearrangement was catalysed by diazabicyclo[2.2.2]octane and second-order rate constants for this process followed a Hammett σ relationship with a ρ value of +0.90. Isotope effects in H_2O- and D_2O-based media for PhCOCHO and PhCOCDO, respectively, were measured at 30 °C to give $k_{max.}$ (H/D) = 5.9 ± 0.9; K_h (H/D) = 0.24 ± 0.08. Activation parameters were obtained for isolated $k_{max.}$ and K_h terms for phenylglyoxal with mercaptoethanol. The data obtained, along with literature information, allowed assignment of the rate-determining step to base-catalysed deprotonation at the C(1)–H site of the hemithioacetal (*i.e.* at the carbon α to the sulphur atom).

The glyoxalase system, discovered in 1913, consists of two enzymes and their cofactor glutathione (GSH). Glyoxalase I (lactoylglutathionelyase, EC 4.4.1.5) converts the hemithioacetal (**1**) formed between GSH and α-oxoaldehydes into *S*-hydroxyacylglutathiones. These thiolesters are then hydrolysed under the catalytic influence of glyoxalase II (hydroxyacylglutathione hydrolase, EC 3.1.2.6) to produce α-hydroxyacids and regenerate GSH [equation (1)].

Glyoxalase I is intriguing not only because inhibitors of it may have anticancer activity[1,2] but also because of its mechanism of action, long cited as a rare example of an enzyme-catalysed hydride transfer but now regarded as more likely[3–7] to be a proton transfer, involving a carbanionic enediolate species (**2**) [equation (2)]. The non-enzymatic rearrangement of α-oxohemithiolacetals, related to (**1**), to thiolesters analogous to (**3**) is a general base-catalysed process.[7–9] The nature of the rate-determining step in the enzymic rearrangement of (**1**) to (**3**) needs clarification. The enzyme-catalysed reaction follows Hammett σ values[10] using literature data for the yeast enzyme with *para*-substituted arylglyoxals. There is also some confusion in the literature about the actual value of the isotope effect in the non-enzymic reaction.[11]

There are a number of other rearrangements of the type shown in equation (3), *e.g.* the intramolecular Cannizzaro rearrangement of arylglyoxals to mandelates,[12–21] aldose–ketose isomerisations (*e.g.* the Lobry de Bruyn–Alberda van Ekenstein rearrangement[22]), the α-ketol rearrangement.[23] The most thoroughly studied is the intramolecular Cannizzaro reaction which occurs by a [1,2] hydride shift,[12–19] although there has been some suggestion of a free-radical route.[20,21] These alternative systems provided a further incentive for the present study.

Accordingly, we present here a study of the non-enzymatic rearrangement, to thiolesters, of the hemithiolacetals formed between 2-mercaptoethanol and a series of substituted arylglyoxals (**5**).

Experimental

Substituted acetophenones, substituted phenacyl halides, mercaptoethanol, 1,4-diazabicyclo[2.2.2]octane (DABCO), and

Table 1. Characterisation of arylglyoxal hydrates, $XC_6H_4C(O)CH(OH)_2$

X	ν C=O[a]/cm^{-1}	^{13}C chemical shift δ(p.p.m., relative to Me_4Si)
4-NO_2	1 688	90.0[d,$CH(OH)_2$]; 195.3(s,C=O); 149.9(s), 138.6(s), 130.8(d), 123.5(d), (aromatics)
4-CF_3	1 693	90.8[$CH(OH)_2$]; 195.6(C=O); for aromatics, see text
3-F	1 696	89.7[$CH(OH)_2$]; 195.6(C=O); for aromatics see text
4-Br	1 692	89.6[d,$CH(OH)_2$]; 195.4(s,C=O); 132.6(d), 131.4(d), 127.2(s), 130.7(s) (aromatics)
4-Cl	1 690	89.6[d,$CH(OH)_2$]; 195.3(s,C=O); 132.3(s), 131.2(d), 130.6(s), 128.5(d) (aromatics)
4-CH_3	1 685	89.1[d,$CH(OH)_2$]; 195.8(s,C=O); 143.7(s), 131.0(d), 129.5(s), 129.0(d) (aromatics); 21.2(q,CH_3)
4-CH_3O	1 678	82.2[d,$CH(OH)_2$]; 197.1(s,C=O); 165.7(s), 133.6(d), 127.4(s), 115.8(d) (aromatics); 57.2(q,CH_3O)

[a] For hydrated ketone determined in a Nujol mull.

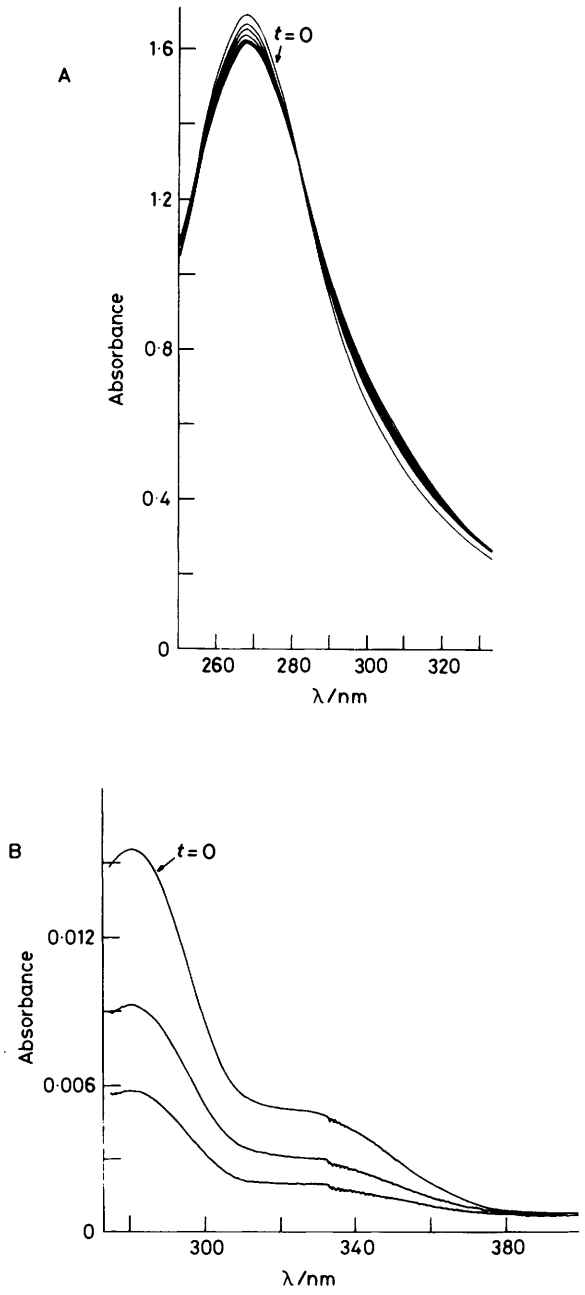

Figure 1. Repetitive spectral scans of the rearrangement of the hemithioacetals from arylglyoxals and mercaptoethanol in 0.2M-DABCO buffer (pH 9.2, 50% free base, μ = 0.5M) at 30.2 °C. A, 4-Nitrophenylglyoxal, cycle time 30 s; B, 4′-trifluoromethylphenylglyoxal, cycle time 360 s

selenious acid were obtained from Aldrich Chemical Co. and used without further purification for synthesis. Phenylglyoxal hydrate (Sigma Chemical Co.) was purified before kinetic use by several recrystallisations from chloroform–acetone as described.[19] Mercaptoethanol (Me) was purified by distillation and stored under nitrogen. [^{2}H]Phenylglyoxal (PhCOCDO, [^{2}H]PG) was a gift from Professor S. Shinkai.

The substituted phenylglyoxals used in this study were synthesised according to literature procedures,[19] usually by selenious acid oxidation of the appropriate acetophenone.[24] As m.p.s are somewhat variable for arylglyoxal hydrates[18,19] the materials were characterised using ^{1}H and ^{13}C n.m.r. along with i.r. spectroscopy (for ^{13}C n.m.r. data see Table 1) and mass spectroscopy. Under the broad-band decoupling conditions used, protons were decoupled but C-F coupling was still clearly seen allowing ready spectral assignments with the assistance of proton coupling. For *m*-fluorophenylglyoxal hydrate under proton-decoupled conditions the following peaks were obtained for aromatic carbon atoms: δ 136.0, 136.3 (C-1, J_{CF} 6.85 Hz), 120.1, 121.2 (C-2, J_{CF} 21.4 Hz), 156.2, 168.4, (C-3, J_{CF} 246 Hz), 115.6, 116.7, (C-4, J_{CF} 22.6 Hz), 130.9, 131.3 (C-5, J_{CF} 7.66 Hz), and 125.9 p.p.m. (C-6, not split by F). For 4-trifluoromethylphenylglyoxal hydrate the following aromatic carbon resonances were detected under proton-decoupled (but fluorine-coupled) conditions: δ 137.1 (C-1, s), 130.2 (C-2, -6, s), 124.1, 125.2, 126.8 (C-3, -5, q, J_{CF} 17.7 Hz), 133.3, 131.7, 131.4, 128.9 (C-4, q, J_{CF} 29.8 Hz), and 117.0 p.p.m. (CF_3, s); CF coupling not detected. In the mass spectrometer the parent peak did not correspond to the hydrate. The highest observable peak was the parent less 17 or 18. From the parent aldehyde CHO loss (*m/e* 29) was followed by CO loss as a general splitting pattern for arylglyoxals.

Buffers were prepared from DABCO using doubly distilled, degassed (using N_2 bubbling) water and contained 10^{-4}M-EDTA to minimise metal-ion interference by oxidative action on mercaptoethanol in the buffer. Buffer solutions were prepared immediately before use and flushed with nitrogen following the method of Okuyama *et al.*[9] Concentrations of mercaptoethanol in the buffers used were assayed after Ellman.[25] For kinetic studies DABCO buffer {[1.5 ml, 0.4M-DABCO (total), 50% free, μ = 0.5M]} plus thiol solution (1.5 ml, 10^{-4}M-EDTA, 10% v/v CH_3CN, μ = 0.5M) were mixed, stoppered under N_2 with rubber septum caps, and allowed to equilibrate in the thermostatted cuvette holder for 15 min. Reaction was initiated by injection of phenylglyoxal (30 μl, 0.013M in water), mixing, and following the resultant absorbance change with time.

A Philips PW9409 digital pH meter was used after standardisation. Kinetic studies were conducted using a Pye–Unicam SP 8, 100 u.v.–visible spectrophotometer with cuvette holder thermostatted by means of water circulating from a Churchill thermoregulator bath. Unless otherwise stated kinetics were studied at 30.2 °C by the method of Okuyama *et al.*[9] using 280 nm to monitor the progress of the rearrangement

(the kinetic wavelength used for the 4-NO_2 derivative was 268 nm). Repetitive spectral scanning of the 4-NO_2 derivative showed a tight isosbestic point at 282 nm, with no drifting (Figure 1A). In contrast, the 4-CF_3 derivative showed no isosbestic point (Figure 1B).

Kinetic runs were started by the addition of a small portion (typically 30 μl) of arylglyoxal hydrate in acetonitrile to DABCO buffer solutions containing appropriate concentrations of β-mercaptoethanol (0.001—0.01M) at fixed pH (usually *ca.* 9.30). After a short time (corresponding to hemithioacetal formation) the absorbance at 280 nm decreased smoothly with time following pseudo-first-order kinetics: k_{obs} (pseudo-first-order rate constants) were obtained from semilogarithmic plots which were linear to greater than two half-lives. Great care was taken to work under anaerobic conditions to prevent drifting of the end-point caused by thiol (or thiolester) oxidation.

To study isotope effects (k_H/k_D) phenylglyoxal was investigated in H_2O-based buffers and deuteriophenylglyoxal (PhCOCDO) in D_2O-based buffers under anaerobic conditions. For D_2O runs buffers were prepared from DABCO free base plus standardised DCl in D_2O. Small aliquots (6–30 μl) of strong standardised mercaptoethanol solutions in D_2O were added to 3.0 ml of D_2O-based DABCO buffer in cuvettes through rubber septum caps to give appropriate final [RSD] levels. Kinetic runs were initiated after equilibration by addition of $PhCOCD(OD)_2$ in D_2O (30 μl of 0.013M) at 30.2 °C. Runs in H_2O media for the isotope effect studies were effected under analogous conditions following an identical protocol.

N.m.r. spectra were run on a Bruker WP 805Y spectrometer (80 MHz for ^1H; 20.15 MHz for ^{13}C). Mass spectra were run on an MS12 mass spectrometer with VG electronics update.

Results

In DABCO buffer (total [DABCO] held constant at 0.2M, 50% free base, ionic strength 0.5M held by KCl, 5% acetonitrile, v/v) values of k_{obs} showed saturation dependence on β-mercaptoethanol (ME) concentration, and the data obeyed equation (4),

$$k_{obs} = k_{max.}K_h[ME]/(1 + K_h[ME]) \quad (4)$$

in agreement with reports of previous workers.[9] Values of $k_{max.}$ and K_h were extracted using least-squares linear regression analysis of the doubly reciprocal form of the data, according to equation (5).

$$\frac{1}{k_{obs}} = \frac{1}{K_h \cdot k_{max.}} \cdot \frac{1}{[RSH]} + \frac{1}{k_{max.}} \quad (5)$$

A typical example of a saturation plot is shown in Figure 2 for 4-chlorophenylglyoxal with β-mercaptoethanol at 30.2 °C. Values of $k_{max.}$ and K_h for the series of arylglyoxals with β-mercaptoethanol at 30.2 °C are collected in Table 2, along with values of k_o and k_{DABCO} from equation (6) which holds[9] at high thiol concentrations.

$$k_{obs} = k_o + k_{DABCO}\,[DABCO] \quad (6)$$

The temperature dependences of $k_{max.}$, K_h, and $k_{max.}K_h$ terms were obtained by measuring complete k_{obs} *versus* [mercaptoethanol] profiles at constant [DABCO] at 29.9, 35.2, 40.1, and 45.6 °C for phenylglyoxal. Kinetic parameters ($k_{max.}$ and K_h) were separated as described above. The plots of ln (kinetic parameter) *versus* $1/T$ were linear (although rather scattered for K_h) and the activation parameters obtained are recorded in Table 3.

Figure 3 shows plots of k_{obs} *versus* ME concentration for $PhCOCH(OH)_2$ in H_2O-based DABCO media and for

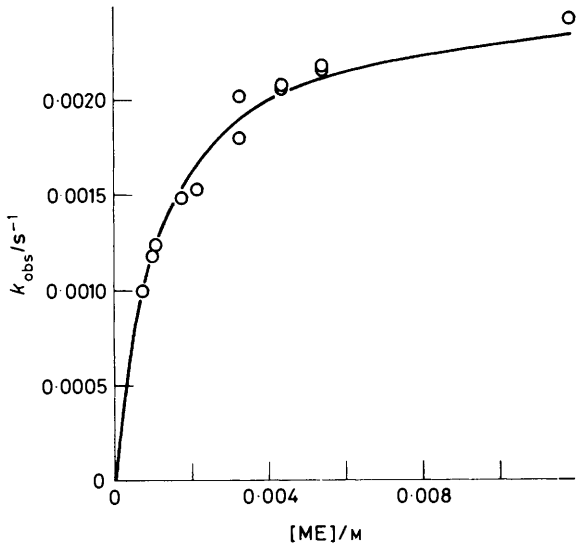

Figure 2. Plot of k_{obs} *versus* mercaptoethanol concentration ([ME]) for rearrangement to thiolester of the hemithioacetal formed between mercaptoethanol and 4-chlorophenylglyoxal in 0.2M-DABCO buffer, ionic strength 0.5M (held with KCl), 50% free base at 30.3 °C. Points are experimental: line is theoretical from equation (4) with $k_{max.} = 2.54 \times 10^{-3}$ s^{-1} and $K_h = 888$ l mol^{-1}

$PhCOCD(OD)_2$ in D_2O-based DABCO buffers at 30.2 °C (0.2M DABCO total, 50% free base, $\mu = 0.5$M). Double-reciprocal forms of these data were used to extract appropriate kinetic parameters. Kinetic parameters and isotope effect data are summarised in Table 4.

In Figure 4 the data for $k_{max.}$, omitting the point for the 4-CH_3O derivative, are shown as a Hammett plot using Hammett σ values [see equation (7)]. The correlation was poorer if the CH_3O point was included (standard deviation on slope ±0.07: $r = 0.985$).

$$\log_{10} k_{max.} = 0.92\,(\pm 0.06)\,\sigma - 2.77\,(r = 0.991) \quad (7)$$

Using Hammett σ^- values gave a significantly poorer correlation $r = 0.932$, standard deviation on slope ±0.09 if all points were used; standard deviation on slope ±0.07, $r = 0.948$ if the 4 CH_3O was excluded). Clearly, the correlation is with Hammett σ values.

The data for DABCO catalysis (k_{DABCO}) also obeyed a Hammett σ correlation [equation (8)].

$$\log_{10}(k_{DABCO}) = 0.90\,\sigma - 1.93\,(r = 0.990) \quad (8)$$

Discussion

In the absence of glyoxalase I the rearrangements, to thiolesters, of hemithioacetals formed from phenylglyoxal and thiols have been suggested to proceed *via* a proton-transfer mechanism based on (a) the incorporation of solvent-derived deuterium into the product,[7,9] (b) flavin-mediated trapping of an intermediate (presumably the carbanion),[26] and (c) the observation of general base catalysis.[7,9] The saturation dependence of rate on thiol concentration was used by Okuyama *et al.*,[9] to show that the hemithioacetal was on the reaction pathway [equation (9)]. They found that formation constants (K_h) for hemithioacetalisation measured under kinetic and equilibrium (spectrophotometrically) conditions were identical. Thus $k_{max.}$ refers to the rearrangement step(s). The process described by the term, $k_{max.}$, is general base-

Table 2. Kinetic parameters for rearrangement, to thiolester, of the β-mercaptoethanol-derived hemithioacetals of substituted arylglyoxals $XC_6H_4C(O)CH(OH)_2$ at 30 °C in degassed 0.2M-DABCO (total) buffer (50% free base), ionic strength held with KCl and in the presence of 5% v/v acetonitrile and 10^{-4}M EDTA[a]

X	σ	$10^3 k_{max.}$ s^{-1}	K_h/l mol^{-1}	$k_{max.}K_h$/l mol^{-1}	$10^4 k_o$/s^{-1}	$10^2 k_{DABCO}$/l mol^{-1} s^{-1}
4-NO_2	0.78	9.25 ± 0.87	475 ± 88	4.39 ± 0.82	14.2 ± 6.8	5.70 ± 0.04
4-CF_3	0.54	4.86 ± 0.34	791 ± 142	3.84 ± 0.41	8.84 ± 4.82	3.51 ± 0.33
3-F	0.34	4.14 ± 0.67	265 ± 77	1.10 ± 0.14	6.62 ± 2.67	2.45 ± 0.19
4-Br	0.23	2.67 ± 0.13	1 655 ± 428	4.42 ± 0.94		2.15 ± 0.06
4-Cl	0.23	2.54 ± 0.08	888 ± 67	2.26 ± 0.10	7.38 ± 1.96	1.96 ± 0.14
H	0.00	1.78 ± 0.12	788 ± 129	1.40 ± 0.14		
4-CH_3	−0.17	1.21 ± 0.18	705 ± 232	0.851 ± 0.154		
4-CH_3O	−0.27	0.656 ± 0.047	771 ± 151	0.505 ± 0.062		

[a] Data collected at ionic strength 0.5M, at a fixed β-mercaptoethanol concentration of 0.005M.

Table 3. Activation parameters for DABCO-catalysed rearrangements, to thiolester, of the hemithioacetal from β-mercaptoethanol and phenylglyoxal. Apart from temperature, conditions were as in Table 2 (standard deviations given in parentheses)

T/°C	$10^3 k_{max.}$/s^{-1}	K_h/l mol^{-1}	$k_{max.}K_h$/ l mol^{-1} s^{-1}
29.9	1.75 ± 0.11	830 ± 125	1.45 ± 0.13
35.2	2.70 ± 0.20	508 ± 71	1.37 ± 0.09
40.1	4.36 ± 0.24	421 ± 40	1.84 ± 0.07
45.6	6.27 ± 0.34	397 ± 37	2.49 ± 0.10
$\Delta H^{\ddagger}$/kcal mol^{-1}	15.9 ± 0.7	−8.90 ± 2.50	6.99 ± 2.35
$\Delta S^{\ddagger}$/cal K^{-1} mol^{-1}	−20.8 ± 2.3	−76.80 ± 8.1	−37.0 ± 7.6
$\Delta G^{\ddagger}$/kcal mol^{-1}	15.3 ± 0.7	−9.50 ± 2.50	6.39 ± 2.35

Table 4. Kinetic isotope data at 30.2 °C for $PhCOCH(OH)_2$ and $PhCOCD(OD)_2$ with mercaptoethanol in H_2O- and D_2O-based buffers, respectively. The buffers used were 0.2M-DABCO total, 50% free base, 0.5M ionic strength (held with KCl)

Medium parameter k	PG/H_2O	$[^2H]PG/D_2O$	k_H/k_D
$10^3 k_{max.}$/s^{-1}	3.47 ± 0.17	0.585 ± 0.056	5.9 ± 0.9
K_h/l mol^{-1}	453 ± 38	1 887 ± 441	0.24 ± 0.08
$k_{max.}K_h$/l mol^{-1} s^{-1}	1.58 ± 0.06	1.10 ± 0.15	1.4 ± 0.7

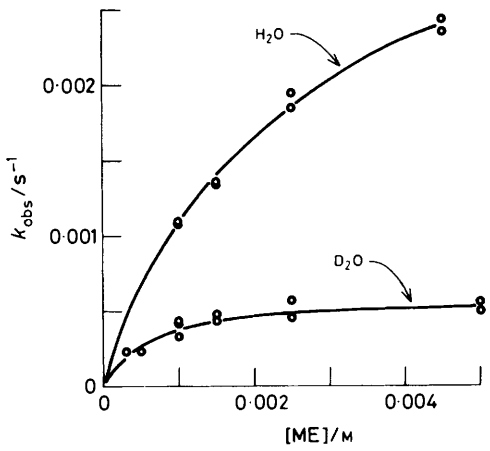

Figure 3. Plots of k_{obs} *versus* mercaptoethanol concentration ([ME]) for phenylglyoxal in H_2O-based buffer (DABCO) and for deuteriophenylglyoxal (PhCOCDO) in D_2O-based buffer (DABCO); see text for details. Points are experimental; lines are calculated using equation (4) and data from Table 4

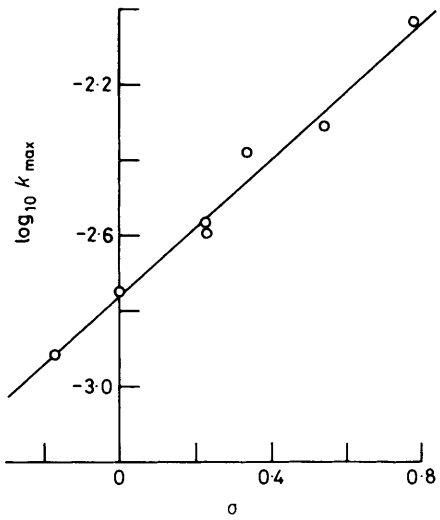

Figure 4. Hammett plot of $\log_{10}$ ($k_{max.}$) *versus* σ values. Points are experimental; the line was obtained by least-squares linear regression analysis of the data in Table 2 with omission of the 4-MeO point

catalysed[9] and in this study we found that for $k_{max.}$ the ρ value for DABCO catalysis was +0.90 with a fit to Hammett σ values, indicating that resonance stabilisation of the transition state does not occur. For the hydride-ion-transfer mechanism of the rearrangement of arylglyoxal hydrates in base [$ArCO{\cdot}CH(OH)O^- \longrightarrow ArCH(OH)CO_2^-$] Vander Jagt *et al.*[19] reported a fit to Hammett σ constants with a ρ value of +2.0. This is a considerably higher value in line with a difference in mechanism for the hydrates and hemithiolacetals. Both hydride-transfer (**6**) and proton-transfer (**7**) transition states involve transfer of negative charge from C_α to C_β, giving rise to positive ρ values. Clearly the change in charge in going to the transition state for the hydrate (with a 'full' H^- transfer) is greater (*cf.* ρ values) than for the hemithioacetal (with its partial proton transfer to produce a π-delocalised state). This argument assumes that the rate-determining step for the hemithioacetal is deprotonation at C_α, as proposed by Okuyama *et al.*[9] (further discussion of this aspect follows later).

Further evidence of a difference in mechanisms for the hemithiolacetal rearrangement and that of aryglyoxals in base is that flavin trapping of a carbanionic intermediate was successful in the former but not the latter system.[26]

Flavins are very inefficient hydride traps[26] (H_2CO–HO^-, BH_4^- systems) and the observation of trapping both in model systems and for yeast glyoxalase itself[6] for the hemithioacetals argues against a hydride ion pathway such as equation (10) with

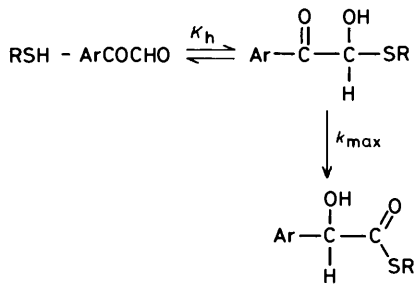

(9)

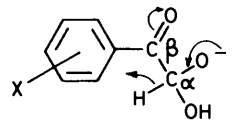

(6)

hydride transfer

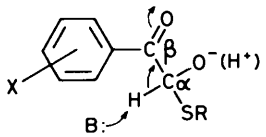

(7)

proton transfer

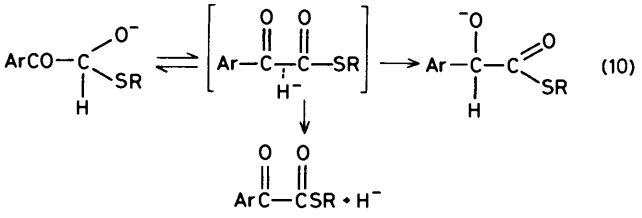

(10)

an encounter complex* which can undergo solvent-deuterium exchange (to explain ^{2}H-incorporation into product from solvent) or conversion into product conjugate base faster than escape of H^- ion into the medium.

Details of the Proton-transfer Mechanism.—The Scheme shows a detailed summary of the relationships between the species likely to participate in a proton-transfer mechanism for the rearrangement of (**8**) to (**16**). In the k_1 step, (**8**) is deprotonated by general base catalysis at C_α to give a resonance-stabilised ('enediolate') carbanion (**9**) ⟷ (**10**). To generate product from this ion, reprotonation must occur at C_β, necessitating a series of (presumably diffusion-controlled)[27] proton transfers at oxygen. The most likely species for C_β reprotonation to give product are (**14**) and (**12**). The enediol (**11**) is analogous to ascorbic acid which has pK_a values of 4.25 and 11.79 for formation of mono- and di-anions, respectively.[28] If the acidities of the hydroxy groups of (**11**) are comparable to ascorbic acid (**14**) would be the vastly predominant species at pH *ca.* 9.2 (*i.e.* in 50% free base DABCO buffers).

Clearly k_3 would have to be *ca.* 10^8-fold greater than k_2 for the majority of the reaction flux to pass through (**12**) and (**15**). However, if k_3 were to be the rate-determining step, one would expect a correlation of $k_{max.}$ with Hammett σ^- values, contrary to observation.

Thus, the good correlation of $k_{max.}$ ($\equiv k_{DABCO}$) with Hammett σ-values argues against significant contribution of species with a negative charge on the oxygen atom at C_α [*i.e.* (**12**), (**14**)] to the rate-controlling transition state.

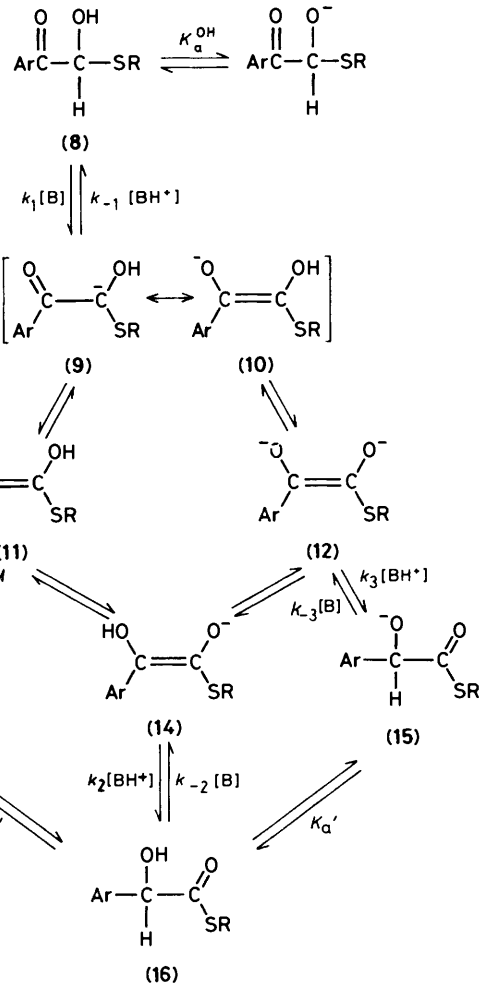

Scheme.

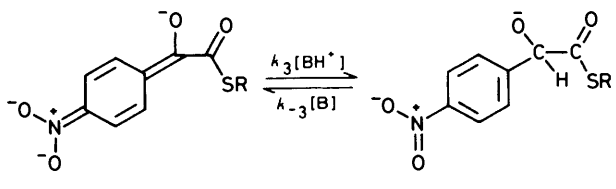

(12) (13)

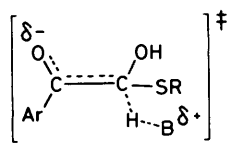

(17)

The σ-correlation could implicate the k_1 step as rate-determining or rate processes involving proton transfer at oxygen (OH) for species (**11**). The latter possibility is unlikely because transfers involving heteroatoms are usually diffusion-controlled[27] and the pK_a of the OH group will presumably be of the order of 4 [*cf.* the ionisation of ascorbic acid[28] with (**11**) ⇄ (**14**)] which is much less than the pK_a of the DABCO buffer (9.2) used. In addition, proton transfers involving the OH site of (**11**) would not show a large primary isotope effect when

*Dr. A. Williams, University of Kent, raised the suggestion that deuterium uptake from solvent need not, *in principle*, imply a proton-exchange mechanism but could support *hydride*-exchange also, given a number of kinetic provisos such as those above.

PhCOCHO and PhCOCDO are compared. In the present study the isotope effect on $k_{max.}$ was 5.9 ± 0.9 (CHO in H_2O compared with CDO in D_2O). Finally, there is no significant kinetic *solvent* isotope effect[9] on $k_{max.}$ [$k_{max.}$ (H/D) 0.9, CHO in H_2O compared with CHO in D_2O], further substantiating this view.

The most straightforward interpretation of the data (σ correlation, primary isotope effect) is that deprotonation at C_α (k_1) is the rate-determining step for the general base-catalysed rearrangement of hemithioacetals formed from β-mercaptoethanol and arylglyoxals to the corresponding α-hydroxyacylthioesters (**17**).

The value of −20.8 cal mol^{-1} K^{-1} for $\Delta S^{\pm}$ ($k_{max.} \equiv k_{DABCO}$) is in broad agreement with the negative values usually obtained for bimolecular processes. It is not yet clear whether the hemithiolacetal OH group is ionised during this process (see K_a^{OH} in the Scheme). In this case (−O$^-$ form) ground state and transition state would possess the same facility for resonance stabilisation by appropriate 4-substituents in the aryl site, which would cancel each other, leading to a σ-correlation. It would be easier for a base to abstract a carbon-bound proton if the site were initially neutral rather than anionic, supporting (**17**) as the transition state. On the enzyme it is possible, of course, that the anionic (at oxygen) hemithioacetal is the active form of the substrate which suffers C_α-H deprotonation by an active-site base. For glyoxalase I, it is known that a zinc ion is located at the active site, not far from the hemithioacetal OH locus and this might assist stabilisation by charge neutralisation of the −O$^-$ form of the hemithioacetal during the early deprotonation stages, perhaps even through an intervening water molecule. Later reprotonation at C_β by the same protonated active-site base requires a full negative charge on the oxygen at C_α and presumably a conformational change of the enzyme is required to decomplex this −O$^-$ from Zn^{2+}.

Acknowledgements

We are grateful to the Cancer Research Campaign (K. T. D.) and to the Turkish Ministry of National Education (H. D.) for support as well as to Dr. A. Williams for helpful discussions.

References

1 R. Vince and W. B. Wadd, *Biochem. Biophys. Res. Commun.*, 1969, **35**, 593
2 A. Szent-Gyorgyi, *Science*, 1968, **161**, 988.
3 S. S. Hall, A. M. Doweyko, and F. Jordan, *J. Am. Chem. Soc.*, 1976, **98**, 7960.
4 J. W. Kozarich, R. V. J. Chari, J. C. Wu, and T. L. Lawrence, *J. Am. Chem. Soc.*, 1981, **103**, 4593.
5 R. V. J. Chari and J. W. Kozarich, *J. Biol. Chem.*, 1981, **103**, 4593.
6 K. Ueda, S. Shinkai, and K. T. Douglas, *J. Chem. Soc., Chem. Commun.*, 1984, 371: K. T. Douglas, S. Shinkai, A. J. Quilter, and K. Ueda, *Biochim. Biophys. Acta*, 1985, **829**, 119.
7 S. S. Hall, A. M. Doweyko, and F. Jordan, *J. Am. Chem. Soc.*, 1978, **100**, 5934.
8 S. S. Hall and A. Poet, *Tetrahedron Lett.*, 1970, 2867.
9 T. Okuyama, K. Kimura, and T. Fueno, *Bull. Chem. Soc. Jpn.*, 1982, **55**, 1493.
10 D. L. Vander Jagt, L.-P. B. Han, and C. H. Lehman, *Biochemistry*, 1972, **11**, 3735.
11 K. T. Douglas and S. Shinkai, *Angew. Chem., Int. Ed. Engl.*, 1985, **24**, 31.
12 E. R. Alexander, *J. Am. Chem. Soc.*, 1947, **69**, 289.
13 E. Doering, T. I. Taylor, and E. F. Schoenwaldt, *J. Am. Chem. Soc.*, 1948, **70**, 455.
14 O. K. Neville, *J. Am. Chem. Soc.*, 1948, **70**, 3500.
15 H. Fredenhagen and F. Bonhoeffer, *Z. Phys. Chem.*, 1938, **A181**, 379.
16 F. H. Westheimer, *J. Am. Chem. Soc.*, 1936, **58**, 2209.
17 A. R. Gray and R. C. Fuson, *J. Am. Chem. Soc.*, 1934, **56**, 739.
18 J. Hine and G. F. Koser, *J. Org. Chem.*, 1971, **36**, 3591.
19 D. L. Vander Jagt, L.-P. B. Han, and C. H. Lehmann, *J. Org. Chem.*, 1972, **37**, 4100.
20 J. Weiss, *Trans. Faraday Soc.*, 1941, **37**, 782.
21 S. K. Chung, *J. Chem. Soc., Chem. Commun.*, 1982, 480.
22 J. Hine, 'Physical Organic Chemistry,' McGraw-Hill, New York, 1962, pp. 271—272.
23 J. March, 'Advanced Organic Chemistry,' McGraw-Hill, New York, 1977, p. 988.
24 H. A. Riley and A. R. Gray, *Org. Synth.*, 1943, Coll. Vol. II, 509.
25 G. L. Ellman, *Arch. Biochem. Biophys.*, 1959, **82**, 70.
26 S. Shinkai, T. Yamashita, Y. Kusano, and O. Manabe, *J. Am. Chem. Soc.*, 1981, **103**, 2070.
27 M. Eigen, *Angew. Chem., Int. Ed. Engl.*, 1964, **3**, 14.
28 G. W. Hay, B. A. Lewis, and F. Smith in 'The Vitamins,' eds. W. H. Sebrell, Jr., and R. S. Harris, Academic Press, New York, 1967, 2nd. edn., vol. 1, p. 308.

Received 4th March 1985; *Paper* 5/363